New Phytologist

Research

Hydraulic redistribution of soil water by roots affects whole-stand evapotranspiration and net ecosystem carbon exchange

Jean-Christophe Domec[1], John S. King[1], Asko Noormets[1], Emrys Treasure[2], Michael J. Gavazzi[2], Ge Sun[2] and Steven G. McNulty[2]

[1]Department of Forestry and Environmental Resources, North Carolina State University, Raleigh, NC 27695, USA; [2]Southern Global Change Program, USDA Forest Service, Raleigh, NC 27606, USA

Author for correspondence:
Jean-Christophe Domec
Tel: +1 919 515 9490
Email: jdomec@ncsu.edu

Received: *16 December 2009*
Accepted: *21 February 2010*

New Phytologist (2010) **187**: 171–183
doi: 10.1111/j.1469-8137.2010.03245.x

Key words: lobolly pine (*Pinus taeda*), overstory, root sap flow, soil water content, understory, water potential.

Summary

- Hydraulic redistribution (HR) of water via roots from moist to drier portions of the soil occurs in many ecosystems, potentially influencing both water use and carbon assimilation.
- By measuring soil water content, sap flow and eddy covariance, we investigated the temporal variability of HR in a loblolly pine (*Pinus taeda*) plantation during months of normal and below-normal precipitation, and examined its effects on tree transpiration, ecosystem water use and carbon exchange.
- The occurrence of HR was explained by courses of reverse flow through roots. As the drought progressed, HR maintained soil moisture above 0.15 cm^3 cm^{-3} and increased transpiration by 30–50%. HR accounted for 15–25% of measured total site water depletion seasonally, peaking at 1.05 mm d^{-1}. The understory species depended on water redistributed by the deep-rooted overstory pine trees for their early summer water supply. Modeling carbon flux showed that in the absence of HR, gross ecosystem productivity and net ecosystem exchange could be reduced by 750 and 400 g C m^{-2} yr^{-1}, respectively.
- Hydraulic redistribution mitigated the effects of soil drying on understory and stand evapotranspiration and had important implications for net primary productivity by maintaining this whole ecosystem as a carbon sink.

Introduction

In addition to water loss through the canopy by transpiration, some plants may also lose water at night through their roots (Richards & Caldwell, 1987). This process, called hydraulic redistribution (HR), involves passive transfer of water from moist to drier portions of the soil profile via roots (Richards & Caldwell, 1987; Caldwell *et al.*, 1998; Burgess & Bleby, 2006). While the water potential gradient required for HR is passive, the roots may not passively lose water, as HR is limited by root cavitation (Warren *et al.*, 2007). Recent studies suggest that as soil water deficits increase, nocturnal fluxes of water associated with HR are sufficient to significantly delay further drying of the upper portion of the soil profile by replacing > 20% of the water utilized during the day with water taken up by roots deeper in the soil profile (Brooks *et al.*, 2002; Meinzer *et al.*, 2004; Amenu & Kumar, 2007). Consequently, HR helps maintain soil water content in a range that prevents soil water potential from dropping to critical values that would cause root hydraulic failure by cavitation (Domec *et al.*, 2004; Warren *et al.*, 2007; Siqueira *et al.*, 2009). The rhizosphere and roots are the most vulnerable components to drought along the soil-to-leaf continuum (Jackson *et al.*, 2000; Domec *et al.*, 2009a), so avoidance of hydraulic failure through HR plays a major role in the success of species growing under a wide range of precipitation and therefore soil moisture regimes (Dawson, 1996; Bauerle *et al.*, 2008). Furthermore, recent numerical studies have shown that the daily replacement of transpired water by HR can potentially affect land-surface climatology (Lee *et al.*, 2005; Siqueira *et al.*, 2009). Therefore, the linkages between soil moisture dynamics and rainfall imply that HR may serve as a mechanism for the interaction between deep layer soil moisture

and regional climate dynamics. Although HR has been reported in a wide variety of ecosystems (Burgess *et al.*, 2000; Jackson *et al.*, 2000; Brooks *et al.*, 2002; Bayala *et al.*, 2008), quantitative understanding of its direct significance for whole-stand water balance and productivity is only beginning to emerge.

General circulation models coupled with climate change experiments predicted that in North America, climate change will result in increases in temperature, decreases in precipitation, higher evapotranspiration (Lenihan *et al.*, 2008), and lower soil water (Gregory *et al.*, 1997). Therefore, the southern USA is likely to be characterized by longer and drier summers that may negatively influence forest productivity (Eamus, 2003; Battles *et al.*, 2008). There are extensive managed forests across the southern coastal plain characterized by highly organic soils (Trettin *et al.*, 1995) that remain one of the few understudied ecosystems of the USA. Our recent work indicates that although evapotranspiration of these pine ecosystems is very sensitive to declining soil water content and to higher evaporative demand (Domec *et al.*, 2009a; Noormets *et al.*, 2010; Sun *et al.*, 2010), net ecosystem exchange does not decline as much as comparable upland plantations (Stoy *et al.*, 2006). Despite limited range, these coastal plain forests act as a strong carbon sink and thus contribute significantly to the regional and continental carbon cycles (Noormets *et al.*, 2010).

The rich soils of these coastal ecosystems tend to be very porous and very water-permeable (Diggs, 2004). Comparable to coarse sand, these histic-mineral soils are characterized by large pore spaces that reduce capillarity. Consequently soil water content and hydraulic conductivity are lost rapidly upon drying, and water extraction operates at high (less negative) water potentials (Campbell, 1985). This was reflected in a greater decrease in predawn tree water potential at higher soil water content in clay soils (Domec *et al.*, 2009b) compared with histic-mineral soils (Domec *et al.*, 2009a). In addition, the highly hydrophobic character of these organic soils may create some air-dried portions of the profile (Heiskanen, 1995) that could compromise their ability to retain water following rain events. Taken together, these soil physical characteristics indicate that to avoid complete desiccation in the upper organic layer, trees growing on histic-mineral soil may rely on deep roots and HR to supply water needs during drought conditions.

The objective in the present study was to evaluate the effect of hydraulic redistribution by roots on plant water use and carbon sequestration in a stand where the role of water as a constraining factor for forest productivity is predicted to increase with climate change. Because plant-level water cycling and ecosystem carbon exchange are intimately coupled (Eamus, 2003), any factor enhancing root water uptake and tree water use is expected to increase carbon uptake and to contribute to higher stand productivity. Thus a basic understanding of how water availability interacts with prevailing water demand is required for quantifying the potential of forest plantations to store carbon in an economically and environmentally sustainable manner (Law *et al.*, 2000; Chen *et al.*, 2004). Forests in the southeastern USA experienced a prolonged dry period during the 2007 and 2008 growing seasons. During these episodes, nearly continuous eddy covariance measurements of CO_2 and water vapor fluxes as well as plant and soil water status were monitored in a mid-rotation loblolly pine (*Pinus taeda*) plantation. These data along with direct estimates of tree transpiration were used to examine the temporal variability of soil moisture and HR, as well as the partitioning of understory and overstory water use. The field data were also used to test a hydraulic model to calculate transpiration and carbon uptake in the presence and in the absence of HR. We hypothesize that, during drought, HR plays a critical role in maintaining the water transport capacity of trees, and in contributing to the high productivity reported for such sites, keeping them as strong carbon sinks.

Materials and Methods

Site description

The study site was a 18-yr-old loblolly pine (*Pinus taeda* L.) plantation located at 35°48′N, 76°40′W on the lower coastal plain of North Carolina, USA (Table 1; Noormets *et al.*, 2010). The area is < 5 m above sea level, on deep Belhaven series histic-mineral soil and belongs to the outer coastal plain mixed forest province. The organic horizon is *c.* 30 cm deep followed by an organic-sandy layer from 30 to 60 cm in depth and by a sandy-loam layer from 60 to 120 cm. The mean (1971–2000) annual precipitation for this site is 1320 mm, the mean temperature in July is 26.6°C, and that in January is 6.4°C. The maximum projected leaf area index (LAI) during the growing season was 4.2 m^2 m^{-2} and decreased to 3.1–3.3 m^2 m^{-2} in winter, mostly as a result of leaf fall of subdominant and understory species (Domec *et al.*, 2009a; Tables 1, 2a). To partition LAI between the overstory pine trees and the understory plants, we measured the seasonal change in leaf loss in 30 litter traps (0.18 m^2 laundry baskets suspended on PVC tubes 15 cm about the forest floor). The litter was collected every 6 wk during spring and summer, and every 2 wk during autumn and early winter. The samples were separated into needles, leaves, and twigs, and these were oven-dried at 65°C for 48 h. The total leaf mass collected during the year, divided by the area of the litter baskets, provided an estimate of annual leaf litter mass production per square meter. For the pine trees, this needle mass was converted to LAI using an averaged value of specific leaf area (SLA) determined from needles harvested from the bottom, middle and

Table 1 Stand characteristics for the 18-yr-old loblolly pine (*Pinus taeda*) plantation

Overstory tree species	*Pinus taeda*
Canopy height (m)	18
Density (trees ha^{-1})	635
Precipitation (mm yr^{-1})	820–950
LAI overstory pine trees (m^2 m^{-2})	3.3–4.2
LAI understory plants (m^2 m^{-2})	0.7
Maximum rooting depth overstory (cm)	185 ± 7
Maximum rooting depth understory (cm)	55 ± 4
Soil organic layer depth (cm)	60 ± 5
% fine roots (< 1.5 mm)	92 ± 4
% roots between 0 and 65 cm	81 ± 3
Total RAI[a] (m^2 m^{-2})	10.4 ± 1.6
RAI 5–30 cm	4.7 ± 0.3
RAI 30–60 cm	3.6 ± 0.2
RAI 60–120 cm	2.1 ± 0.9
RAI 0–1 mm	8.5 ± 0.7
RAI 1–2 mm	1.2 ± 0.3
RAI > 2 mm	0.7 ± 0.1
K_s (cm h^{-1})[b]	27 ± 9
Bulk soil density 5–65 cm (g cm^{-3})	1.0 ± 0.1
Bulk soil density 60–120 cm (g cm^{-3})	1.3 ± 0.2
E (mm yr^{-1})	695–742
E_t (mm yr^{-1})	1011–1225
GEP (g C m^{-2} yr^{-1})	2480–2910
–NEE[c] (g C m^{-2} yr^{-1})	360–835
ER (g C m^{-2} yr^{-1})	2050–2120
SR[d] (g C m^{-2} yr^{-1})	1081–1219

LAI, leaf area index; RAI, root area index by soil layer depth and root size classes (n = 4 excavated soil pits); K_s, saturated soil hydraulic conductivity; E, annual (2007–08) pine tree transpiration; E_t, whole-stand evapotranspiration; GEP, gross ecosystem productivity; NEE, net ecosystem exchange; ER, ecosystem respiration; SR, soil respiration.
[a]RAI between each of the three soil layers was different at $P < 0.05$ (paired t-test).
[b]Diggs (2004).
[c]NEE values are negative.
[d]Noormets *et al.* (2010).

top parts of the canopy. For the understory species, the dry leaf biomass was multiplied by the average SLA determined on the main nine species present at the site to obtain an estimate of understory LAI (see Table 2b for species list). For each species, SLA was determined as the ratio of projected leaf area to leaf-blade dry mass on at least 15 leaves per species (Garnier *et al.*, 2001).

Microclimate and eddy covariance measurements

The following micrometeorological parameters were measured above canopy: relative humidity and air temperature (HMP45AC, Vaisala, Finland), photosynthetic photon flux density (PPFD; LI-190, Li-Cor, Lincoln, NE, USA) and precipitation (TE-525, Campbell Scientific, Logan, UT, USA). Water and carbon fluxes between the forest canopy and atmosphere were measured using eddy covariance. The 23 m tower was located in the middle of the 1 km^2 stand and instrumented with an open-path infrared gas analyzer (IRGA; LI-7500, Li-Cor) and a three-dimensional sonic anemometer (CSAT3; Campbell Scientific). The 30 min mean fluxes of H_2O were calculated as the covariance of vertical wind speed and the concentration of H_2O, representing the total water loss, including soil evaporation and canopy interception. As previously reported for this type of ecosystem (Novick *et al.*, 2009), nocturnal evapotranspiration represented < 10% of daily water fluxes. The 30 min mean fluxes of CO_2 were computed as the covariance of vertical wind speed and the concentration of CO_2 and were corrected for the warming of the IRGA (Burba *et al.*, 2008) and for fluctuations in air density (Webb *et al.*, 1980). Net daily ecosystem exchange (NEE, g C m^{-2} d^{-1}) of CO_2 represents an integration of photosynthesis, plant dark respiration, and soil respiration and was calculated as the sum of turbulent flux and change in CO_2 storage in the canopy air space (Noormets *et al.*, 2007). During the night, there is no photosynthetic uptake, so daily ecosystem respiration (ER, g C m^{-2} d^{-1}) can be considered the source of the entire net carbon flux. Therefore, ER was directly measured as the night-time flux, restricted to periods of PPFD < 4 mmol m^{-2} s^{-1}. Data were screened for periods of precipitation and dew, low turbulence and wind direction (Noormets *et al.*, 2007, 2010). Finally, daily average gross ecosystem productivity (GEP, g C m^{-2} d^{-1}) of CO_2 was determined by the equation GEP = −NEE + ER.

Soil water content

Soil water probes consisted of multiple annular capacitance sensors (Sentek Pty Ltd, Adelaide, Australia) separated vertically by 10 cm or more, placed in weatherproof PVC access tubes. These probes are relatively insensitive to fluctuations in soil temperature (Warren *et al.*, 2005). Two probes were installed to a depth of 1.4 m, with eight independent sensors per probe. Each sensor was calibrated from soil cores taken at each sensor depth (Domec *et al.*, 2009a). Soil water storage, measured in millimeters of water within a specified layer of soil, was calculated by summing the volumetric water content (θ) for each 10 cm sensor within that layer. When there was a vertical gap between sensors, such as between 80 and 100 cm, and between 100 and 140 cm, the intervening layer was interpolated as an average of the sensors above and below the gap. Total daily water use was calculated as the difference between the maximum and minimum soil water storage measured within a 24 h period. Net HR (in mm d^{-1}) was defined as the nightly increase in θ, and was calculated as the difference between the minimum θ of one day and the maximum θ of the next day (Brooks *et al.*, 2002; Warren *et al.*, 2007). Soil water depletion and HR were not estimated on the day following rain events. In addition to the Sentek probes, θ was also measured

Table 2 (a) Overstory (loblolly pine (*Pinus taeda*) trees) and understory projected leaf area index; and (b) leaf transpiration rates and specific leaf area (SLA) represented by the main tree species

	Leaf area index			
	August	September	October	December
(a)				
Loblolly pine	4.2	4.0	3.6	3.4
Understory plants	0.7	0.4	0.2	< 0.1

	Transpiration (mmol m^{-2} s^{-1})[a]				
	August	September	October	December	SLA (m^2 kg^{-1})[a]
(b)					
Loblolly pine (*Pinus taeda*)	1.6 ± 0.2	1.2 ± 0.1	1.0 ± 0.1	0.8 ± 0.1	5.9 ± 0.8
Understory plants					
Red maple (*Acer rubrum*)	2.1 ± 0.1	2.8 ± 0.4	2.4 ± 0.3	N/A[b]	31.5 ± 3.8
Pokeweed (*Phytolacca americana*)	6.8 ± 0.5	4.5 ± 0.5	1.1 ± 0.1	N/A	21.0 ± 2.0
Devil's walking stick (*Aralia spinosa*)	2.5 ± 0.4	0.2 ± 0.1	N/A	N/A	15.1 ± 0.5
American holly (*Ilex opaca*)	3.9 ± 0.4	3.1 ± 0.3	3.9 ± 0.5	0.6 ± 0.2	7.5 ± 0.3
Muscadine vine (*Vitis rotundifolia*)	5.7 ± 0.1	3.2 ± 0.1	2.8 ± 0.8	N/A	26.4 ± 1.1
Beautyberry (*Callicarpa americana*)	3.0 ± 0.4	2.3 ± 0.5	2.1 ± 0.1	N/A	30.0 ± 4.0
Redbay (*Persea borbonia*)	3.0 ± 0.4	2.1 ± 0.5	2.6 ± 0.4	N/A	12.9 ± 1.4
Giant cane (*Arundinaria macrosperma*)	5.1 ± 0.5	3.9 ± 1.0	1.5 ± 0.3	0.4 ± 0.1	20.0 ± 1.0
Meadow grass (*Poa* spp.)	5.2 ± 0.7	2.3 ± 0.5	N/A	N/A	28.3 ± 1.7
Understory plants/all plants[c] (%)	28	18	8	2	

[a]One-side (projected) leaf area values were used to calculate transpiration and SLA.
[b]N/A denotes the dates when transpiration measurements were not possible due to leaf availability.
[c]Understory plants/all plants represents the transpiration of the understory plants as a percentage of all plant transpiration (overstory plus understory).

over the top 30 cm of the soil profile using two vertically inserted CS616 time domain reflectometers (Campbell Scientific). The depth of the water table was monitored with a pressure water level data logger (Infinities, Port Orange, FL, USA). Predawn leaf water potential ($\Psi_{predawn}$) was measured every 3–4 wk from May 2007 to December 2008 during nights of low vapor pressure deficit (Dawson *et al.*, 2007) to obtain an integrated measure of the soil water potential in the root volume. Predawn water potential was measured on four different trees and on three needles per tree using a pressure chamber (PMS Instruments, Albany, OR, USA).

Transpiration

Unlike the eddy correlation technique, which measures total evapotranspiration, the sap flow method only measures tree transpiration (E) and does not account for water loss from understory plants. We measured sap flux density per unit of conducting xylem area (J_s, g m^{-2} s^{-1}) in stem xylem of seven trees. Stem sap flux measurements were made at 1.4 m above the ground at four radial positions using 20 mm heat dissipation probes (Granier, 1987). Preliminary results showed that there was no significant difference in azimuthal J_s within trees (P = 0.39, Student's paired t-test), probably as a result of the homogeneity of pine trunks, so we inserted all probes on the north-north-west side of the trees. Thirty-minute averages of temperature difference data were computed and stored in data loggers (CR10; Campbell Scientific). The sensor signal was converted to J_s, according to Granier (1987) and accounted for the effects of nonzero night-time fluxes on the signal baseline by using nights with low vapor pressure deficit to estimate maximum temperature differences on nights with nocturnal transpiration (Oishi *et al.*, 2008). Using tree sapwood area and stand tree density (Table 1), J_s was scaled and converted to a tree-scale average transpiration per unit ground area (E, in mm d^{-1}). The total sapwood area of the trees equipped with sap flow probes was estimated from the relationship between sapwood area and diameter determined on 22 felled trees, and the diameter of the measured trees. Further details on the sap flow method at this site can be found in Domec *et al.* (2009a).

To understand the contribution of overstory water use to overall stand water use, hand-held measurement of stomatal conductance and transpiration was determined on the most common species using a steady-state porometer (Li-1600; Li-Cor). The porometer was equipped with a conifer chamber for the pine trees (Li-1600-02). Measurements were taken on four trees per species between 09:00 and 13:00 h on two consecutive sunny days in August, September, October and December 2008.

Root sap flow

To detect the relative influence of transpiration and HR on root sap flow, we selected two trees for root sap flow measurement between May and September 2008. Root sap flow was measured with the same thermal dissipation technique used to determine tree transpiration modified to permit the direction of flow to be detected (Brooks *et al.*, 2002, 2006; JR Brooks & R Coulombe, unpublished). In its original form, the thermal dissipation technique measures only unidirectional flow. However, for each root we installed a directional probe which allows the thermal dissipation method to detect reversal of flow. A heated temperature sensor, 10 mm in length, was inserted into the xylem in the centre of the exposed root. Two unheated reference temperature sensors (10 mm in length) were placed axially 100 mm up- and downstream from the heater sensor and wired to measure the temperature differences between the heated and unheated sensors. For the directional probe, two thermocouples were inserted 9 mm axially to a depth of 7 mm up- and downstream from the heated probe (Brooks *et al.*, 2002). The movement of the heated water raised the temperature of the downstream thermocouple relative to that of the upstream thermocouple, providing an accurate gauge to direction of flow. The temperature of the reference probe that was determined to be upstream of the direction of flow was used to calculate root J_s. At the time when the flux probe signal reached its daily maximum (zero flow), the directional probe value was very close to zero, and we used that value to differentiate between upward and reverse flow in the root.

Model application of water use

To estimate values of E that would have occurred without HR, we used the hydraulic transport model developed by Sperry *et al.* (1998). This model has previously given good predictions of water use in *P. taeda* (Ewers *et al.*, 2000; Hacke *et al.*, 2000). The model also predicts the upper boundary for steady-state water transport as a function of soil water potential (Ψ_s), which represents the plant's 'water use envelope' (termed critical transpiration). Once E exceeds the critical transpiration, there cannot be any further water uptake because of irreversible hydraulic dysfunction in the soil–leaf hydraulic pathway (Sperry *et al.*, 2002). From the hydraulic properties of soil and xylem, the model solves the relationship between steady-state E and the driving force in the soil–plant continuum ($E = K_l(\Psi_s - \Psi_l)$), where K_l is the leaf-specific hydraulic conductance, and $\Psi_s - \Psi_l$ is the water potential difference between soil and leaf (Ψ_l). The drop in Ψ in the continuum is used to calculate the reduction in K_l from the rhizosphere drying, root and stem cavitation, and to determine E.

The water potential-dependent decrease in rhizophere conductance was calculated from soil conductivity (K_s), soil texture and Ψ_s assuming a cylindrical rhizosphere sheath of 5 mm thickness from bulk soil to root surface (for details, see Sperry *et al.*, 1998). The initial saturated K_s value was taken at 27 cm h^{-1} (415 mol $s^{-1}MPa^{-1}m^{-1}$), a parameter that was measured at the same site (Diggs, 2004; Table 1). To convert rhizosphere conductance to a ground area basis, we needed an estimate of the all-sided fine root area index (RAI). Because root production is generally highest during late spring and early summer (King *et al.*, 2002), we excavated four 1.1-m-deep, 1 × 1 m pits in June–July 2009 and sampled roots every 20 cm to determine change in root distribution and surface area with depth (Table 1). We sorted roots by diameter into three classes (< 1, 1–2, > 2 mm) and determined the total dry mass of each size class. Root area was calculated from the total dry mass and from the relationships between dry mass and root area (specific root area) calculated from 75 randomly selected roots (Table 1). Fine RAI showed an exponential decrease with soil depth (cm) (RAI = $0.27e^{-0.02 \times \text{depth}}$, $R^2 = 0.98$) with 79% of the roots found in the upper 0–60 cm (Table 1). In addition, excavation of five tree stumps revealed that deep roots were located up to 1.8 ± 0.2 m depth.

Soil water potential was calculated from Campbell (1985) as:

$$\Psi_s = \Psi_e(\theta/\theta_s)^{-b} \qquad \text{Eqn 1}$$

where Ψ_e is the soil water potential at air entry, θ_s is the saturated volumetric water content and the exponent b is related to soil texture. We used $b = 5.2$, $\Psi_e = 0.3$ kPa, and $\theta_s = 0.62$ m^3 m^{-3}, for the 0–30 cm soil layer; $b = 3.7$, $\Psi_e = 0.6$ kPa, and $\theta_s = 0.52$ m^3 m^{-3} for the 30–60 cm soil layer; and $b = 3.8$, $\Psi_e = 1.0$ kPa, and $\theta_s = 0.37$ m^3 m^{-3} for the 60–120 cm soil layer. All these parameters were derived by fitting Eqn 1 to moisture-release data from the site (Diggs, 2004).

Based on early work at the site (Domec *et al.*, 2009a), the initial saturated K_l was taken as 0.85 mmol m^{-2} s^{-1} MPa^{-1} and the root and stem components were assumed to comprise 55% and 45% of K_l, respectively. Midday Ψ_l was measured with the pressure chamber on the same days as $\Psi_{predawn}$. Root and shoot systems were further divided into lateral and axial components. For the root systems, axial and lateral root components were split into three soil layers (0–30, 30–60 and 60–120 cm). The water potential-dependent decrease in xylem hydraulic conductance was calculated from a Weibull function fit to the root or stem vulnerability curve data ($R^2 > 0.92$, $P < 0.001$). Vulnerability curves were determined using the air injection technique (Sperry & Saliendra, 1994) on six roots and six branches collected in February–March 2008. We used the same fitting parameters for axial and lateral components within the root and shoot systems.

We parameterized the model to simulate K_l and transpiration rates using Ψ_s under normal field conditions (that included HR) and using Ψ_s predicted without HR. Modeled transpiration under normal field conditions were compared to measured E derived from sap fluxes for days where the average vapor pressure deficit exceeded 1 kPa (Hacke *et al.*, 2000). Across many forest types, gross carbon uptake has been shown to be directly related to water loss (Law *et al.*, 2000). Therefore, from these modeled transpiration rates with HR and without HR, GEP was calculated using the specific relationship between measured GEP and E we determined at our site (Supporting Information, Fig. S1a). Further, from this estimated GEP with and without HR, NEE was calculated by subtracting ecosystem ER. The effect of HR on ER was modeled using a nonlinear model fit between ER and θ (Fig. S1b). This relationship was best described by a quadratic equation because ER was slightly reduced under dry conditions (Mielnick & Dugas, 2000; Noormets *et al.*, 2008), probably because of low soil respiration resulting from inhibited root and microbial activities (Lin *et al.*, 1999).

Results

Seasonal patterns in soil water content and root HR

The 2007 and 2008 growing seasons experienced an extreme drought, with soil water content (θ) reaching a minimum in late August, and remained depleted until major rain events occurred in late October (Fig. 1a). Mean annual precipitation for the measurement period was 870 mm, which was 65% of the 30 yr mean for the area. At the beginning of the study in April–May 2007, the soil was close to field capacity with the water table at 30 cm below ground, and θ of the 0–120 cm layer ranging from 0.35 to 0.41 $cm^3\ cm^{-3}$ (Fig. 1a). Field capacity was almost reached again in 2008 for the deeper soil layers when rain events caused a transient partial recovery of θ. In June and between August and November, gradual soil drying occurred, with the water table dropping below 1.9 m and θ falling to 0.11 $cm^3\ cm^{-3}$ for the 0–60 cm layer and to 0.19 $cm^3\ cm^{-3}$ for the 60–120 cm layer.

We found that HR was restricted to the upper 70 cm of soil. Early in the season, the total amount of water redistributed was negligible (< 0.05 mm d^{-1}) and began to increase steadily in July, reaching a maximum of 1.1 mm d^{-1} in mid-October. This increase in HR through the season was related to the decrease in θ. On average, from July to October, HR contributed > 0.6 mm d^{-1} and up to 25% of soil water depletion (Fig. 1b), and over the entire year, HR contributed to 10% of whole-year water use. For the days with significant nocturnal transpiration, we found a negative relationship between nocturnal transpiration and HR (data not shown), probably because the tree canopy acted as a competitor with the upper soil for water (Warren *et al.*, 2007).

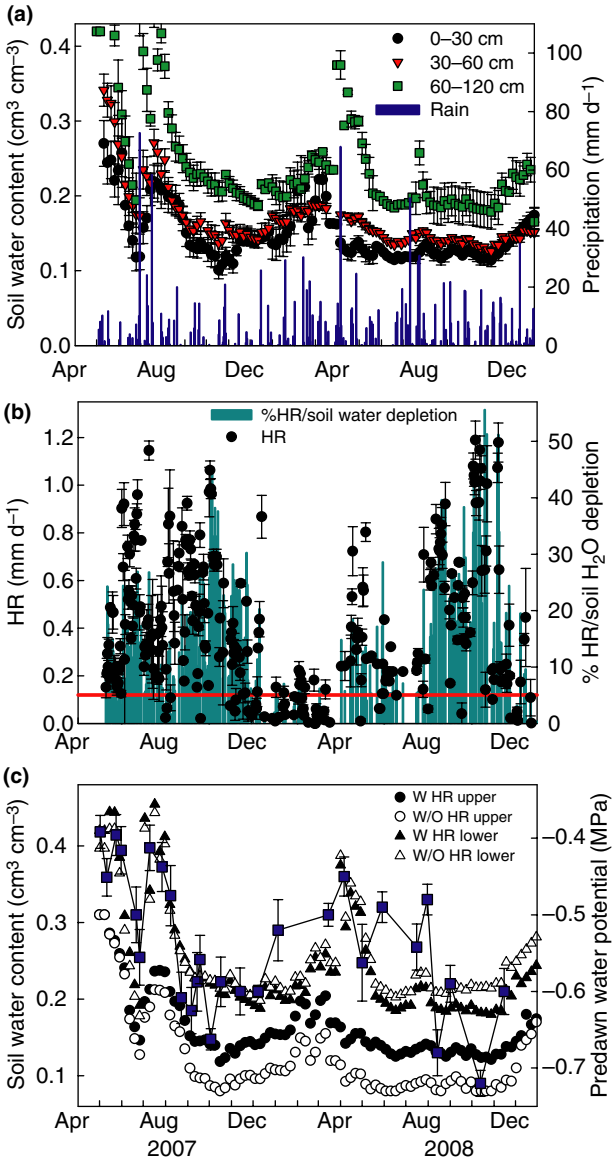

Fig. 1 Seasonal patterns in soil water content and precipitation (a), root hydraulic redistribution (HR) and HR as a percentage of total soil water depletion (b), and soil water content over the upper soil profile (0–60 cm) and the lower soil profile (60–120 cm) with (W) and without (W/O) HR (c). In (b) the horizontal line represents the maximum capillary water rise though soil. In (c) closed squares represent predawn leaf water potentials corrected for gravity to ground level so they are comparable to soil water potentials weighted by root area. Error bars are standard errors (SE).

Liquid transport between soil layers is dependent upon unsaturated soil hydraulic conductivity (K) and the existence of a water potential gradient (Darcy's law). Based on the equations of Campbell (1985) using soil hydraulic parameters and measured saturated K (Table 1), estimates of K for the upper soil were < 6×10^{-6} cm h^{-1} in February and < 1.2×10^{-7} cm h^{-1} in September. Such variability in

K corresponded to a capillary rise of 0.12 mm d^{-1} in February and < 0.01 mm d^{-1} in September, which was in the same order as the increase in HR detected in winter, but was always < 5% of measured HR during the growing season (Fig. 1b). The seasonal decline in $\Psi_{predawn}$ corrected for the gravitational component was very responsive to changes in θ, and as the soil dried, $\Psi_{predawn}$ declined in parallel (Fig. 1c; inset Fig. 2a). By the time θ reached its seasonal minimum value, $\Psi_{predawn}$ had declined to *c.* −0.65 MPa. Compared with the observed change in θ, the predicted values of θ in the absence of HR were greater for the upper soil (0–60 cm) and lower for the lower soil (60–120 cm) (Fig. 1c). The time course deviation of predicted vs observed θ for the upper soil was greatest in late summer when θ would have fallen below 0.1 cm^3 cm^{-3} in the absence of HR (Fig. 1c). However, significant deviation of predicted and observed θ did not occur until $\Psi_{predawn}$ had fallen below −0.55 MPa.

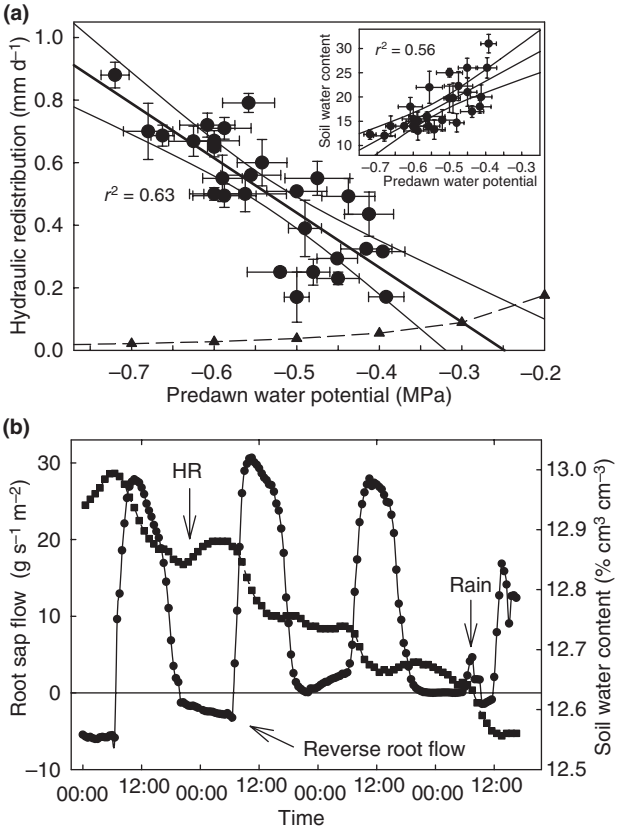

Fig. 2 (a) Hydraulic redistribution as a function of the average predawn water potential (closed circles). Triangles represent the decrease in capillary water rise with declining soil water potentials. The inset in (a) shows the linear relationship between predawn water potential and soil water content. (b) Time courses of sap flow in roots of a loblolly pine (*Pinus taeda*) tree (11–15 August 2008). A positive value means that flow was towards the base of the tree, whereas a negative value indicates reverse flow away from the base of the tree. Circles, root sap flow; squares, soil water content.

Mirroring the seasonal increase in HR with decreasing θ and $\Psi_{predawn}$, HR was also linearly related to the decrease in $\Psi_{predawn}$ (Fig. 2a). The capillary rise through soil was of the same magnitude as HR through roots and was predicted to occur at $\Psi_{predawn}$ of < −0.3 MPa, which corresponded with the lower limit of detected HR (Fig. 2a). The directional probe temperature differential provided additional information to determine when reverse flow was occurring (Fig. 2b). Of the three major lateral roots where root sap flow was monitored, only two showed significant reverse flow over the entire monitoring period. Those roots were located at 25 and 35 cm soil depth. In the roots with reverse flow, the mean nightly transport back to the soil was equivalent to *c.* 15% of the daily transport up the tree, which represented 0.4 kg of water daily. If we assume that most roots experienced backflow, then *c.* 5.0 kg of water was transported back to the soil at night by each tree, since, during the day, the amount of water used by a root represented 8–9% of the water used by the whole tree. The timing of reverse flow was consistent with the timing of the increase in θ during the night (Fig. 2b).

Whole-stand water loss, tree water loss and soil water depletion

To erase the effect of canopy interception and the technical difficulty with rain events, all evapotranspiration (E_t) and soil water depletion data were screened for rainy days. The differences in sap flow estimates of *E* and the eddy correlation technique estimates of E_t (Fig. 3) suggested that understory transpiration was minor during winter and early spring. By contrast, during late spring and early summer, *E* represented only 65% of all stand water loss as a result of the understory effect. The understory vegetation at this site represented *c.* 12–18% of total leaf area and was mostly composed of ephemeral spring shrubs, grasses and young red maple seedlings (Table 2). Hand-held measurement of transpiration on the most common species showed that the understory plants had higher rates of water loss per unit leaf area than the pine trees (Table 2b). Combined with the percentage cover, we estimated that understory vegetation contributed up to 28% of E_t, which was similar to the difference between the ratio of *E* to E_t between winter and summer (Fig. 3).

The amount of water utilized in the upper 1.2 m of soil reached a maximum of 6.1 mm d^{-1}, with an average of 4.2 mm d^{-1} through the summer (Fig. 4a). These rates were consistent with E_t measured with the eddy flux technique (Fig. 4b). Peak rates of soil water depletion were observed through August when precipitation had stopped but $\Psi_{predawn}$ was still near its maximum. During this time, the lower soil layers (60–120 cm) were contributing a similar amount of water to daily water depletion as the upper layers (10–60 cm) (Fig. 5). As θ began to decline and soil

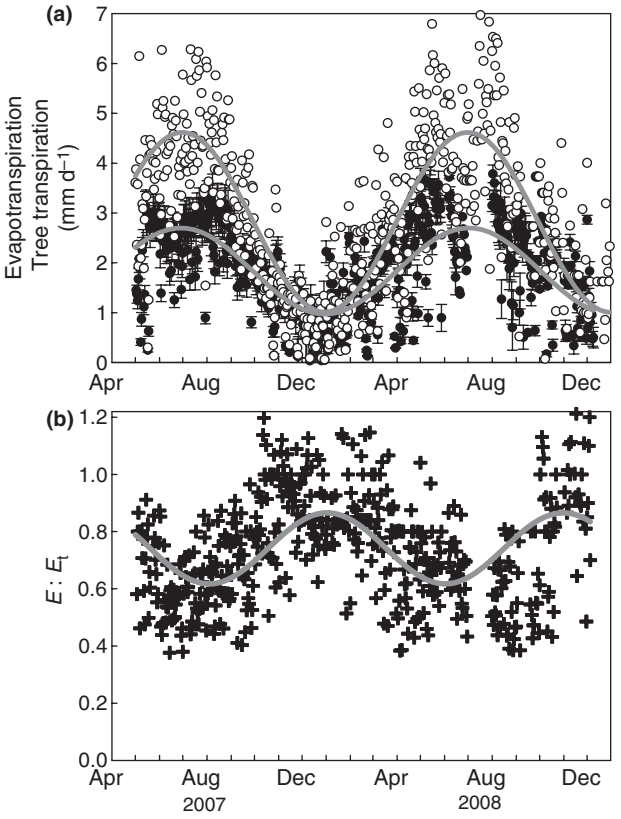

Fig. 3 Comparison between whole-stand water loss and tree water loss (rainy days excluded) showing the seasonal patterns in (a) total evapotranspiration (E_t, open circles) and tree transpiration (E, closed circles), and (b) in the ratio of $E : E_t$. Sinusoidal lines represent the seasonal fitted curves ($R^2 > 0.27$). Although, the variability inherent to both independent methods used made $E : E_t > 1$ in some winter days, the fitted maximum value of $E : E_t$ was equal to 0.87.

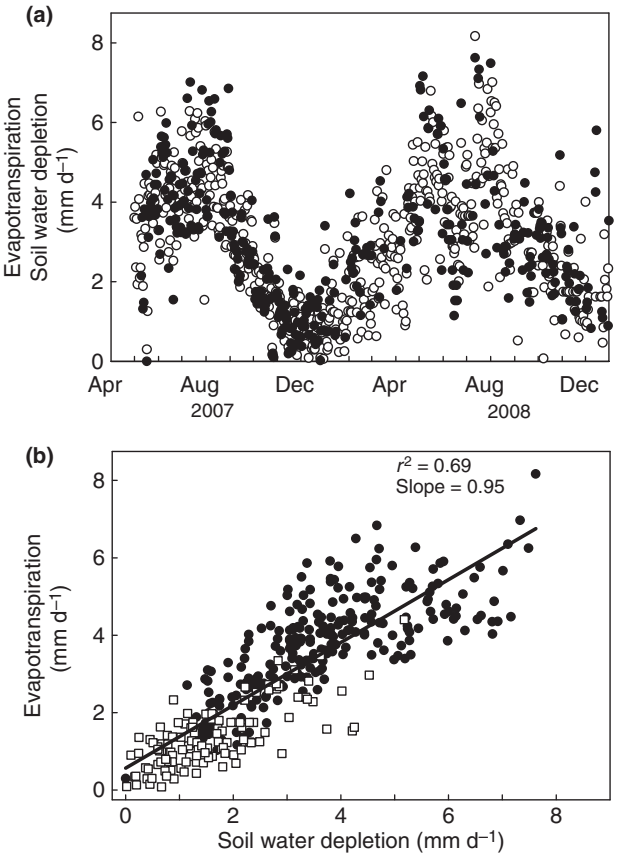

Fig. 4 Seasonal patterns and relationship between whole-stand water loss calculated from eddy flux (evapotranspiration) and from soil water depletion (rainy days excluded). (a): open circles, evapotranspiration; closed circles, soil water depletion; (b), closed circles, summer and autumn; open squares, winter and spring.

water depletion reached its maximum, the contribution of the lower soil to daily water depletion began to increase from 30% in winter and spring to 59% in summer and fall (Fig. 5). In the peak of the summer, the upper soil contributed up to 40% of total water use, which corresponded to *c.* 2.0 mm d^{-1}. Water use from the lower soil reflected water use by the overstory trees only because no understory plant roots were present below 60 cm (Table 1). Owing to the similar estimate of total water use derived from E_t and from soil water depletion (Fig. 4), we determined the partitioning of water use from the upper soil between the understory and the overstory pines. We first calculated the total understory water use as the difference between E_t and E, and then we compared it with the total water depletion of the upper soil that reflected water use by both understory and overstory species. From May to August, most of the water used from the upper soil was by the understory plants. Water used by the understory plants represented up to 30% of the total soil water depletion (Fig. 5), and compared well with the porometry-based partitioning of leaf transpiration (Table 2b; closed symbols in Fig. 5).

Effect of HR on tree transpiration and ecosystem carbon exchange

The hydraulic model yielded accurate estimates of canopy-scale transpiration (Fig. 6) and GEP (Fig. 7). Without HR, transpiration rates would have been closer to critical values of transpiration, increasing the danger of triggering full hydraulic failure by cavitation (Fig. 6). Replacing 25 and 50% of daily soil water use by HR prevented soil water potentials from declining below −0.6 and −0.95 MPa, respectively. Over the seasonal range of field θ and Ψ_s, tree water use would have dropped by > 80% without water redistributed by roots. In addition, the increase in transpiration as a result of HR was proportional (slope not different from 1, $P = 0.001$) to the increase in replacement of soil water by HR (insert of Fig. 6).

Modeled GEP and NEE with HR compared well with measured values (Fig. 7). Following two dry years, cumulative GEP and NEE without HR were predicted to be 1995 and 90 g C m^{-2} yr^{-1}, respectively. Without HR, GEP was very responsive to drought, with a reduction in cumulative GEP of 900 g C m^{-2} in the first year and 600 g C m^{-2} in

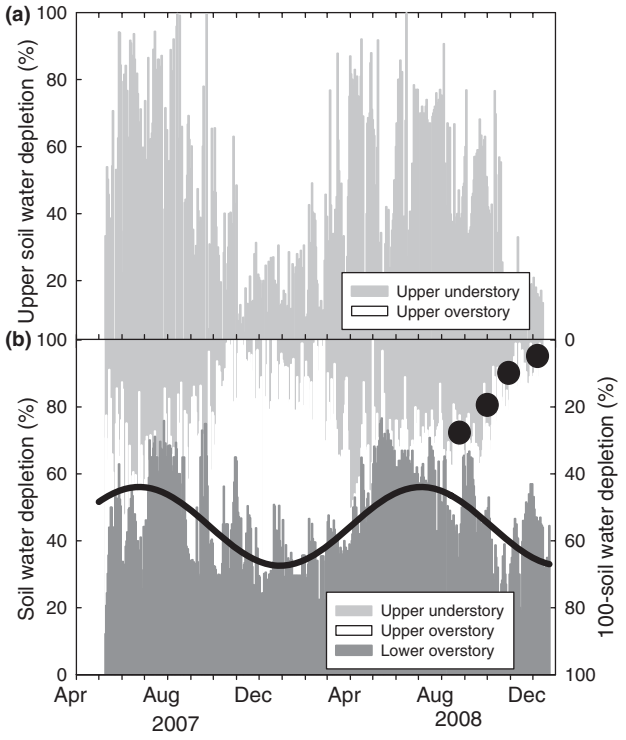

Fig. 5 Seasonal pattern of mean daily water depletion from (a) the upper 10–60 cm and from (b) the lower (60–120 cm) soil profiles. The solid line represents the seasonal fitted curve (R^2 = 0.42). Closed circles represent the measured contribution of understory vegetation to all stand evapotranspiration. The upper soil profile (a) was further divided into overstory and understory water use (upper panel).

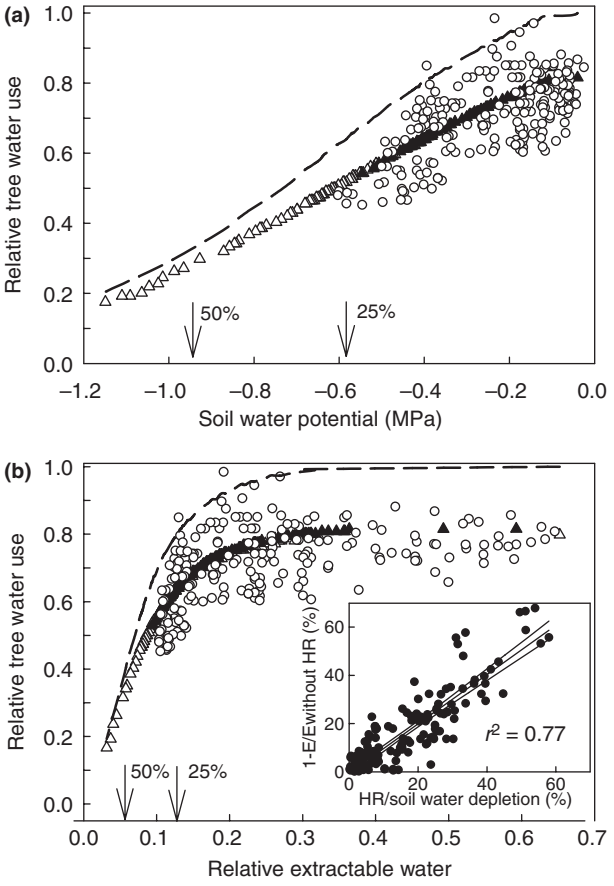

Fig. 6 Measured relative transpiration rate (a) vs soil water potential (Ψ_s) weighted by root area or (b) vs relative soil extractable water for a monotonic decline in Ψ_s (open symbols). The closed and open triangles are the predicted relative tree water use with and without hydraulic redistribution (HR), respectively. The dashed line is the predicted critical relative transpiration rate before irreversible hydraulic failure (Sperry *et al.*, 1998). The arrows represent the values of soil water potentials and relative extractable water that would have been reached without the 25 and 50% daily replacement of soil water by HR. The inset shows the percentage increase in transpiration that would have occurred without HR vs the percentage daily replacement by HR.

the second year (Fig. 7a). When θ was high in spring, monthly rates of −NEE exceeded 100 g C m^{-2}. The θ deficits caused peak rates of CO_2 uptake to decrease. Without HR there would have been a dramatic reduction in the magnitude of NEE, becoming positive by the end of the year. The second year of lower θ maintained the predicted NEE without HR as a carbon source with a reduction in annual carbon sequestration of 400 g C m^{-2}.

Discussion

Partitioning of soil water and magnitude of HR

Our results illustrated the large contribution of deeper roots to water uptake and to HR. In the winter, 65% of the water needed for transpiration was absorbed from the upper soil and water uptake shifted gradually to deeper horizons as water demand increased (Rambal, 1984; Bréda *et al.*, 1995; Warren *et al.*, 2005). When the amount of water utilized daily from the upper soil layers began to decline in late July and early August, the total amount of water hydraulically redistributed to this area began to increase. At the peak of the growing season, the pines replenished the soil water pool each night with 0.7–0.8 mm of groundwater. Comparable with other stands (Emerman & Dawson, 1996; Brooks *et al.*, 2002; Nadezhdina *et al.*, 2006; Warren *et al.*, 2007), this represented > 20% of the previous day's water use. HR continued throughout the dry summer months, suggesting that absorptive surface roots were maintained despite the absence of precipitation. For our soil type and a similar rooting density profile, the numerical simulations of Siqueira *et al.* (2008) would have predicted a maximum HR to occur at θ = 0.23 cm^3 cm^{-3} (from Fig. 9 in Siqueira *et al.*, 2008). This is in good agreement with the value of θ = 0.20 cm^3 cm^{-3} found in this study (Fig. 1b). Furthermore, in many ecosystems, it has been observed that HR began when soil water potential reached *c.* −0.4 to −0.7 MPa

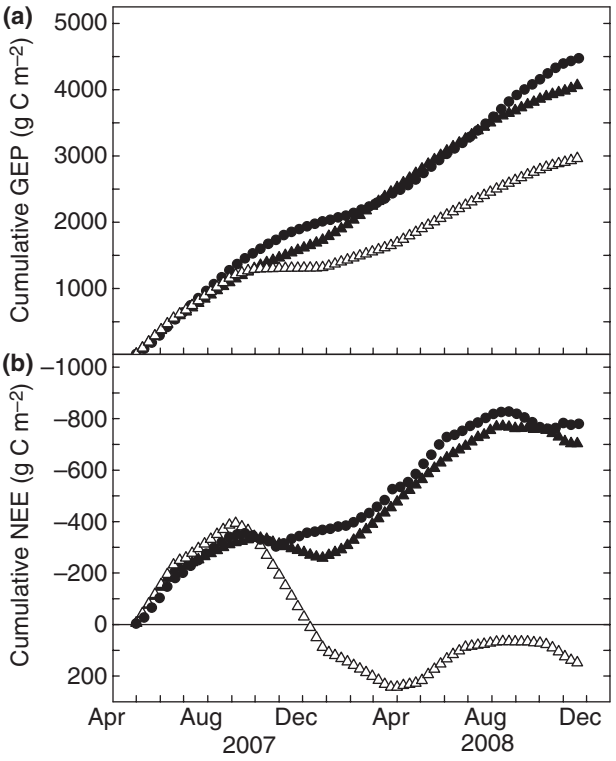

Fig. 7 Measured and modeled cumulative gross ecosystem productivity (GEP) (a) and net ecosystem exchange (NEE) (b) over two growing seasons. Closed triangles, modeled with hydraulic redistribution (HR); open triangles, modeled without HR; circles, measured values.

(Dawson, 1993; Meinzer *et al.*, 2004), which was also roughly equivalent to a $\theta \leq 0.20$ cm^3 cm^{-3} at these sites.

Maintaining root persistence in dry soil by HR has several beneficial implications for the whole plant. During drought periods, HR influences the root–soil interface where steep soil water potential gradients create dry non-conductive zones (Domec *et al.*, 2006; Nadezhdina *et al.*, 2009) leading to lower xylem tension and an increase in root cavitation (Sperry *et al.*, 1998; Domec *et al.*, 2004). Further, such loss of root water transport reduces whole-plant hydraulic conductance and triggers stomatal closure (Domec *et al.*, 2004). Roots of plants that perform HR may also have a faster recovery response following rain events after periods of drought, thus potentially allowing the plant to better compete for water and nutrients (Burgess *et al.*, 2001). Finally, extended root function and lifespan in dry soil may also increase the ability of mycorrhizal fungi to utilize water and nutrients (Warren *et al.*, 2008).

In field studies, HR may be confused with soil capillary rise that takes place independently of roots. Liquid transport between soil layers and within roots is dependent upon soil or root hydraulic conductivity and the existence of a water potential gradient. At this site, root conductance has been shown to decrease by 40% as the soil dries (Domec *et al.*, 2009a), which is relatively minor in comparison with the decline in soil conductivity at water potentials where HR is commonly observed. As the soil dries, the decline in soil unsaturated conductivity is indeed faster than the concurrent decrease in water potential, and therefore liquid water flux through soil is known to approach zero (Siqueira *et al.*, 2008). Despite this decrease in capillary rise as the soil dries, our measured rates of HR increased (Fig. 2a), probably because the rise in the water potential gradients between the root and soil system more than offset the decrease in root hydraulic conductance resulting from embolism (Warren *et al.*, 2007; Scholz *et al.*, 2008). Finally, the onset of HR was also tied to the development of reverse sap flow within roots (Fig. 2b). These considerations lead us to conclude that most of the diurnal fluctuations in soil moisture were root-mediated.

HR impacted overstory and understory water use

We successfully divided transpiration between understory and overstory components for the upper soil. Although understory vegetation comprised only 10–16% of total stand leaf area, understory transpiration represented up to 30% of the total water loss. The understory experiences different environmental conditions because it is relatively sheltered with lower vapor pressure deficit than the overstory (Ishida *et al.*, 1992; Unsworth *et al.*, 2004). During periods of high evaporative demand, such conditions may in fact limit stomatal closure and maintain higher water loss than for the overstory trees (Moore *et al.*, 2004; Jarosz *et al.*, 2008; Stoy *et al.*, 2008).

Although the constant heat sap flux approach is often cited as underpredicting transpiration (Granier *et al.*, 2000; Wilson *et al.*, 2001), there was a good quantitative agreement between sap flux-based tree transpiration and E_t when the overstory pine trees comprised almost 100% of total stand leaf area (Fig. 3). This was probably because of the uniformity of the pine trees reducing between-tree variability, and also because we measured sap flow almost across the entire sapwood depth, thus reducing within-tree uncertainties. Because deciduous angiosperms are leafless during the winter, winter transpiration closely matched total site E_t. The 11–13% differences between tree transpiration and stand E_t during winter (Fig. 3) may be explained by soil evaporation. In closed canopy forest stands with a thick litter layer, soil evaporation is expected to be quite low because of poor coupling with the atmosphere and high resistance to water vapor loss from dry top soil (Granier *et al.*, 2000; Oishi *et al.*, 2008).

The deep-rooted pine trees enabled more efficient extraction of deep-soil water, and there was less shallow water transpired at the peak of the summer, corresponding with the peak of understory plant transpiration. Forest stands composed of both small understory trees and large overstory trees have overlapping root systems that use different water

sources and hence have a greater influence on the hydrologic balance than stands with reduced or no understory (Emerman & Dawson, 1996; Ludwig *et al.*, 2004). The mechanism of HR does not exclude the possibility that the roots releasing the water are of different species than the roots using it later (Dawson, 1993; Filella & Peñuelas, 2003). Roots from the understory plants were not present below 55 cm (Table 1) and thus were only confined within the soil layers where HR was detected. Because, from May to August, understory plants depleted > 70% of the upper soil water (Fig. 5), during this time most of the redistributed water was taken up by the small trees, grasses and shrubs. This provided > 0.5 mm d^{-1} of water and thus probably extended the period over which understory plants could grow. However, later in the season, there was a switch in the partitioning of upper soil water use such that from September to November most of the redistributed water was used by the overstory trees.

Root-mediated HR affected water and carbon balance

Increasing the amount of HR increased the amount of water that was utilized from the soil and prevented the trees from reaching their maximum water extraction limit, analogous to the permanent wilting point (Sperry *et al.*, 2002). Trees were able to operate at less negative Ψ_s and at higher relative extractable soil water than they would without HR (Fig. 6). As a consequence, they were able to extract more soil water, which supports the idea that HR can increase transpiration by a plant (Jackson *et al.*, 2000; Mendel *et al.*, 2002). It should be noted that HR started when θ fell below 0.21–23 m^3 m^{-3}, or 0.20–0.27 relative extractable soil water, which has been shown to correspond to the onset of loss of plant hydraulic conductance and of stomatal closure (Domec *et al.*, 2009a).

We demonstrated that HR impacted carbon balance, allowing the trees to photosynthesize through periods of seasonal drought and maintaining GEP above ER. Total ecosystem carbon uptake at our study site (Table 1) exceeded the average estimates for a coastal oak/loblolly pine forest (180–250 g C m^{-2} yr^{-1}) (Heath *et al.*, 2003), as well as for an upland loblolly pine forest of a similar age (200–600 g C m^{-2} yr^{-1}) (Schäfer *et al.*, 2003; Oren *et al.*, 2006; Stoy *et al.*, 2006). The latter site (Duke Forest) is characterized by a shallow soil with a clay pan on the order of 30–35 cm and a rooting depth of < 60 cm (Oren *et al.*, 1998; Stoy *et al.*, 2006). Such soil and rooting differences probably limited HR and may explain the differences in 20–23% or 500–600 g C m^{-2} yr^{-1} in GEP between both sites; differences that correspond to the modeled increase in GEP with HR (Fig. 7). It is also interesting to note that during the severe drought of 2002, comparable to the summer droughts of 2007 and 2008, one gap-filling scenario predicted that NEE at the Duke site was positive and equal to 20 g C m^{-2} yr^{-1} (Stoy *et al.*, 2006), which is comparable to the 50 g C m^{-2} yr^{-1} predicted by our model if no HR had occurred (Fig. 7b).

Conclusions

This study provided lines of evidence indicating that the capability of roots to redistribute water from deep to shallow soil layers has an important impact on plant-level water cycling and ecosystem carbon exchange. As shown, HR increased dry season (July–October) stand water use by up to 50%. In addition, the overstory species depended on deep-rooted overstory pine trees for their early summer water supply by taking more water from the upper soil horizon than did the trees. Our model indicated that such an increase in transpiration over a 2 yr period affects NEE through major changes in GEP, thereby establishing a direct link between plant root functioning and carbon fluxes. The warming climate is expected to bring along higher vapor pressure deficit, which is likely to increase night-time transpiration. This, in turn, will result in greater soil water demand and lower replenishment of surface soil by HR because trees will act as a competitor with the upper soil for water. All of these may translate to reduced carbon assimilation and sequestration by trees.

Acknowledgements

This study was supported by the USDA Forest Service Southern Global Change Program cooperative agreements 03-CA-11330147-073 and 04-CA-11330147-238. We thank the Weyerhaeuser Company for facilitating access to the study site and offering logistical assistance. John Sperry is gratefully acknowledged for providing the water transport model. We thank Gena Simpson, Duncan Briley, Anna Barnes, and Crystal Garcia for conducting soil-pit digging and root sorting and for assisting with field data collection.

References

Amenu GG, Kumar P. 2007. A model for hydraulic redistribution incorporating coupled soil-root moisture transport. *Hydrology and Earth System Sciences Discussions* **4**: 3719–3769.

Battles JJ, Robards T, Das A, Waring K, Gilless JK, Biging G, Schurr F. 2008. Climate change impacts on forest growth and tree mortality: a data-driven modeling study in a mixed-conifer forest of the Sierra Nevada. *Climatic Change* **87**: 193–213.

Bauerle TL, Richards JH, Smart DR, Eissentat DM. 2008. Importance of internal hydraulic redistribution for prolonging the lifespan of roots in dry soil. *Plant, Cell & Environment* **31**: 177–181.

Bayala J, Heng LK, Van Noordwijk M, Ouedraogo SJ. 2008. Hydraulic redistribution study in two native tree species of agroforestry parklands of West African dry savanna. *Acta Oecologica* **34**: 370–378.

Bréda N, Granier A, Barataud F, Moyne C. 1995. Soil water dynamics in an oak stand. I. Soil moisture, water potentials and water uptake by roots. *Plant and Soil* **172**: 17–27.

Brooks JR, Meinzer FC, Coulombe R, Gregg J. 2002. Hydraulic redistribution of soil water during summer drought in two contrasting Pacific Northwest coniferous forests. *Tree Physiology* **22**: 1107–1117.

Brooks JR, Meinzer FC, Warren JM, Domec JC, Coulombe R. 2006. Hydraulic redistribution in a Douglas-fir forest: lessons from system manipulations. *Plant, Cell & Environment* **29**: 138–150.

Burba GG, McDermitt DK, Grelle A, Anderson DJ, Xu L. 2008. Addressing the influence of instrument surface heat exchange on the measurements of CO_2 flux from open-path gas analyzers. *Global Change Biology* **14**: 1854–1876.

Burgess SSO, Adams MA, Turner MC, White DA, Ong CK. 2001. Tree roots: conduits for deep recharge of soil water. *Oecologia* **126**: 158–165.

Burgess SSO, Bleby TM. 2006. Redistribution of soil water by lateral roots mediated by stem tissues. *Journal of Experimental Botany* **57**: 3283–3291.

Burgess SSO, Pate JS, Adams MA, Dawson TE. 2000. Seasonal water acquisition and redistribution in the Australian woody phreatophyte, *Banksia prinotes*. *Annals of Botany* **85**: 215–224.

Caldwell M, Dawson TE, Richards JH. 1998. Hydraulic lift: consequences of water efflux from the roots of plants. *Oecologia* **113**: 151–161.

Campbell GS. 1985. *Soil physics with BASIC; transport models for soil–plant systems*. Amsterdam, the Netherlands: Elsevier.

Chen J-Q, Paw UKT, Ustin SL, Suchanek TH, Bond BJ, Brosofske KD, Falk M. 2004. Net ecosystem exchanges of carbon, water, and energy in young and old-growth Douglas-fir forests. *Ecosystems* **7**: 534–544.

Dawson TE. 1993. Hydraulic lift and water use by plants: implications for water balance, performance, and plant–plant interactions. *Oecologia* **95**: 565–574.

Dawson TE. 1996. Determining water use by trees and forest from isotopic, energy balance and transpiration analyses; the roles of tree size and hydraulic lift. *Tree Physiology* **16**: 263–272.

Dawson TE, Burgess SSO, Tu KP, Oliveira RS, Santiago LS, Fisher JB, Simonin KA, Ambrose AR. 2007. Nighttime transpiration in woody plants from contrasting ecosystems. *Tree Physiology* **27**: 561–575.

Diggs J. 2004. *Hydrology and nitrogen loading of forested fields in a coastal plain watershed*. MS thesis. North Carolina State University, Raleigh, NC, USA.

Domec J-C, Noormets A, King JS, Sun G, McNulty SG, Gavazzi M, Boggs J, Treasure E. 2009a. Decoupling the influence of leaf and root hydraulic conductances on stomatal conductance and its sensitivity to vapor pressure deficit as soil dries in a drained loblolly pine plantation. *Plant, Cell & Environment* **32**: 980–991.

Domec J-C, Palmroth S, Ward E, Maier CA, Therezien M, Oren R. 2009b. Acclimation of leaf hydraulic conductance and stomatal conductance of *Pinus taeda* (loblolly pine) to long-term growth in elevated CO_2 (free-air CO_2 enrichment) and N-fertilization. *Plant, Cell & Environment* **32**: 1500–1512.

Domec J-C, Scholz FG, Bucci SJ, Meinzer FC, Goldstein G, Villalobos-Vega R. 2006. Diurnal and seasonal variation in root xylem embolism in neotropical savanna woody species: impact on stomatal control of plant water status. *Plant, Cell & Environment* **29**: 26–35.

Domec J-C, Warren JM, Meinzer FC, Brooks JR, Coulombe R. 2004. Native root xylem embolism and stomatal closure in stands of Douglas-fir and ponderosa pine: mitigation by hydraulic redistribution. *Oecologia* **141**: 7–16.

Eamus D. 2003. How does ecosystem water balance affect net primary productivity of woody ecosystem. *Functional Plant Biology* **30**: 187–205.

Emerman SH, Dawson TE. 1996. Hydraulic lift and its influence on the water content of the rhizosphere: an example from sugar maple, *Acer saccharum*. *Oecologia* **108**: 273–278.

Ewers BE, Oren R, Sperry JS. 2000. Influence of nutrient versus water supply on hydraulic architecture and water balance in *Pinus taeda*. *Plant, Cell & Environment* **23**: 1055–1066.

Filella I, Peñuelas J. 2003. Indications of hydraulic lift by *Pinus halepensis* and its effects on the water relations of neighbour shrubs. *Biology Plantarum* **47**: 209–214.

Garnier E, Shipley B, Roumet C, Laurent G. 2001. A standardized protocol for the determination of specific leaf area and leaf dry matter content. *Functional Ecology* **15**: 688–695.

Granier A. 1987. Sap flow measurement in Douglas fir stems using a new thermal method. *Annales Des Sciences Forestieres* **44**: 1–14.

Granier A, Biron P, Lemoine D. 2000. Water balance, transpiration and canopy conductance in two beech stands. *Agricultural and Forest Meteorology* **100**: 291–308.

Gregory JM, Mitchell JFB, Brady AJ. 1997. Summer drought in northern midlatitudes in a time-dependent CO_2 climate experiment. *Journal of Climatology* **10**: 662–686.

Hacke UG, Sperry JS, Ewers BE, Ellsworth DS, Schäfer KVR, Oren R. 2000. Influence of soil porosity on water use in *Pinus taeda*. *Oecologia* **124**: 495–505.

Heath LS, Smith JE, Birdsey RA. 2003. Carbon trends in U.S. forestlands: a context for the role of soils in forest carbon sequestration. In: Kimble JM, Heath LS, Birdsey RA, Lal R, eds. *The potential of U.S. forest soils to sequester carbon and mitigate the greenhouse effect*. Boca Raton, FL, USA: CRC Press, 35–45.

Heiskanen J. 1995. Physical properties of two-component growth media based on sphagnum peat and their implications for plant-available water and aeration. *Plant and Soil* **172**: 45–54.

Ishida A, Yamamura Y, Hori Y. 1992. Roles of leaf water potential and soil-to-leaf hydraulic conductance in water use by understory woody plants. *Ecological Research* **7**: 213–223.

Jackson RB, Sperry JS, Dawson TE. 2000. Root water uptake and transport: using physiological processes in global predictions. *Trends in Plant Science* **5**: 482–488.

Jarosz N, Brunet Y, Lamaud E, Irvine M, Bonnefond J-M, Loustau D. 2008. Carbon dioxide and energy flux portioning between the understorey and the overstorey of a maritime pine forest during a year with reduced soil water availability. *Agricultural and Forest Meteorology* **148**: 1508–1523.

King JS, Albaugh TJ, Allen HL, Buford M, Strain BR, Dougherty P. 2002. Below-ground carbon input to soil is controlled by nutrient availability and fine root dynamics in loblolly pine. *New Phytologist* **154**: 389–398.

Law BE, Waring RH, Anthoni PM, Aber JD. 2000. Measurements of gross and net ecosystem productivity and water vapour exchange of a *Pinus ponderosa* ecosystem, and an evaluation of two generalized models. *Global Change Biology* **6**: 155–168.

Lee J-E, Oliveira RS, Dawson TE, Fung I. 2005. Root functioning modifies seasonal climate. *Proceedings of the National Academy of Sciences, USA* **102**: 17576–17581.

Lenihan JM, Bachelet D, Drapek RJ, Neilson RP. 2008. The response of vegetation distribution, ecosystem productivity, and fire in California to future climate scenarios simulated by the MC1 dynamic vegetation model. *Climatic Change* **87**: 215–230.

Lin G, Ehleringer JR, Rygiewicz PT, Johnson MG, Tingey DT. 1999. Elevated CO_2 and temperature impacts on different components of soil CO_2 efflux in Douglas-fir terracosms. *Global Change Biology* **5**: 157–168.

Ludwig F, Dawson TE, Prins HHT, Berendse F, de Kroon H. 2004. Below-ground competition between trees and grasses may overwhelm the facilitative effects of hydraulic lift. *Ecology Letter* **7**: 623–631.

Meinzer FC, Brooks JR, Bucci S, Goldstein G, Scholz F, Warren J. 2004. Converging patterns of uptake and hydraulic redistribution of soil water in contrasting woody vegetation types. *Tree Physiology* **24**: 919–928.

Mendel M, Hergarten S, Neugebauer HJ. 2002. On a better understanding of hydraulic lift: a numerical study. *Water Resource Research* **38**: 1183.

Mielnick PC, Dugas WA. 2000. Soil CO_2 flux in a tall grass prairie. *Soil Biological and Biochemistry* **32**: 221–222.

Moore GW, Bond BJ, Jones JA, Phillips N, Meinzer FC. 2004. Structural and compositional controls on transpiration in 40- and 450-year-old riparian forests in western Oregon, USA. *Tree Physiology* **24**: 481–491.

Nadezhdina N, Cermak J, Gasparek J, Nadezhdin V, Prax A. 2006. Vertical and horizontal water redistribution within Norway spruce (*Picea abies*) roots in the Moravian Upland. *Tree Physiology* **26**: 1277–1288.

Nadezhdina N, Steppe K, De Pauw DJW, Bequet R, Cermak J, Ceulemans R. 2009. Stem-mediated hydraulic redistribution in large roots on opposing sides of a Douglas-fir tree following localized irrigation. *New Phytologist* **184**: 932–943.

Noormets A, Chen J, Crow TR. 2007. Age-dependent changes in ecosystem carbon fluxes in managed forests in northern Wisconsin, USA. *Ecosystems* **10**: 187–203.

Noormets A, Desai AR, Cook BD, Euskirchen ES, Ricciuto DM, Davis KJ, Bolstad PV, Schmid HP, Vogel CV, Carey EV *et al.* 2008. Moisture sensitivity of ecosystem respiration: Comparison of 14 forest ecosystems in the Upper Great Lakes Region, USA. *Agricultural and Forest Meteorology* **148**: 216–230.

Noormets A, Gavazzi M, McNulty S, Sun G, Domec J-C, King J, Chen J. 2010. Response of carbon fluxes to drought in a coastal plain loblolly pine forest. *Global Change Biology* **16**: 272–287.

Novick K, Oren R, Stoy P, Siqueira M, Katul GG. 2009. Nocturnal evapotranspiration in eddy-covariance records from three co-located ecosystems in the Southeastern U.S.: implications for annual fluxes. *Agricultural and Forest Meteorology* **149**: 1491–1504.

Oishi AC, Oren R, Stoy PC. 2008. Estimating components of forest evapotranspiration: a footprint approach for scaling sap flux measurements. *Agricultural and Forest Meteorology* **148**: 719–732.

Oren R, Ewers BE, Todd P, Phillips N, Katul GG. 1998. Water balance delineates the soil layer in which moisture affects canopy conductance. *Ecological Applications* **8**: 990–1002.

Oren R, Hseih CI, Stoy P, Albertson J, McCarthy HR, Harrell P, Katul GG. 2006. Estimating the uncertainty in annual net ecosystem carbon exchange: spatial variation in turbulent fluxes and sampling errors in eddy-covariance measurements. *Global Change Biology* **12**: 883–896.

Rambal S. 1984. Water balance and pattern of root water uptake by a *Quercus coccifera* L. evergreen shrub. *Oecologia* **62**: 18–25.

Richards JH, Caldwell MM. 1987. Hydraulic lift: substantial nocturnal water transport between soil layers by *Artemisia tridentata* roots. *Oecologia* **73**: 486–489.

Schäfer KVR, Oren R, Ellsworth DS, Lai C, Herricks JD, Finzi AC, Richter DD, Katul GG. 2003. Exposure to an enriched CO_2 atmosphere alters carbon assimilation and allocation in a pine forest ecosystem. *Global Change Biology* **9**: 378–1400.

Scholz FG, Bucci SJ, Goldstein G, Moreira MZ, Meinzer FC, Domec J-C, Villalobos-Vega R, Franco AC, Miralles-Wilhelm F. 2008. Biophysical and life-history determinants of hydraulic lift in Neotropical savanna trees. *Functional Ecology* **22**: 773–786.

Siqueira M, Katul GG, Porporato A. 2008. Onset of water stress, hysteresis in plant conductance, and hydraulic lift: scaling soil water dynamics from millimeters to meters. *Water Resources Research* **44**: W01432.

Siqueira M, Katul GG, Porporato A. 2009. Soil moisture feedbacks on convection triggers: the role of soil–plant hydrodynamics. *Journal of Hydrometeorology* **10**: 96–112.

Sperry JS, Adler FR, Campbell GS, Comstock JP. 1998. Limitation of plant water use by rhizosphere and xylem conductance: results from a model. *Plant, Cell & Environment* **21**: 347–359.

Sperry JS, Hacke UG, Oren R, Comstock JP. 2002. Water deficits and hydraulic limits to leaf water supply. *Plant, Cell & Environment* **25**: 251–263.

Sperry JS, Saliendra NZ. 1994. Intra- and inter-plant variation in xylem cavitation in *Betula occidentalis*. *Plant, Cell & Environment* **17**: 1233–1241.

Stoy PC, Katul GG, Siqueira MBS, Juang J-Y, Novick KA, Uebelherr JM, Oren R. 2006. An evaluation of models for partitioning eddy covariance-measured net ecosystem exchange into photosynthesis and respiration. *Agricultural and Forest Meteorology* **141**: 2–18.

Stoy PC, Katul GG, Siqueira MBS, Yuang J, Novick K, McCarthy HR, Oishi C, Oren R. 2008. Role of vegetation in determining carbon sequestration along ecological succession in the southeastern United States. *Global Change Biology* **14**: 1409–1427.

Sun G, Noormets A, Gavazzi M, McNulty S, Chen J, Domec J-C, King J, Amatya D, Skaggs RW. 2010. Energy and water balance of two contrasting loblolly pine plantations on the lower coastal plain of North Carolina. *Forest Ecology and Management*. doi: 10.1016/j.foreco.2009.09.016

Trettin CC, Jurgensen MF, Gale MR, McLaughlin JW. 1995. Soil carbon in northern forested wetlands: impacts of silvicultural practices. In: McFee WW, Kelly JM, eds. *Carbon forms and functions in forest soils*. Madison, WI, USA: Soil Science Society of America, 437–461.

Unsworth MH, Phillips N, Link T, Bond B, Falk M, Harmon M, Hinckley T, Marks D, Paw U. 2004. Components and controls of water flux in an old-growth Douglas-fir/western hemlock ecosystem. *Ecosystems* 7: 468–481.

Warren JM, Brooks JR, Meinzer FC, Eberhart JL. 2008. Hydraulic redistribution of water from *Pinus ponderosa* trees to seedlings via ectomycorrhizal fungi. *New Phytologist* **180**: 90–99.

Warren JM, Meinzer FC, Brooks JR, Domec JC. 2005. Vertical stratification of soil water storage and release dynamics in Pacific Northwest coniferous forests. *Agricultural and Forest Meteorology* **130**: 39–58.

Warren JM, Meinzer FC, Brooks JR, Domec J-C, Coulombe R. 2007. Hydraulic redistribution of soil water in two old-growth coniferous forests: quantifying patterns and controls. *New Phytologist* **173**: 753–765.

Webb EK, Pearman GI, Leuning R. 1980. Correction of flux measurements for density effects due to heat and water vapor transfer. *Quarterly Journal of the Royal Meteorological Society* **106**: 85–106.

Wilson KB, Hanson PJ, Mulholland PJ, Baldocchi DD, Wullschleger SD. 2001. A comparison of methods for determining forest evapotranspiration and its components: sap-flow soil water budget eddy covariance and catchment water balance. *Agricultural and Forest Meteorology* **106**: 153–168.

Supporting Information

Additional supporting information may be found in the online version of this article.

Fig. S1 Relationships between measured gross ecosystem productivity (GEP) as a function or tree transpiration (a) and ecosystem respiration (ER) as a function of soil moisture (b).

Please note: Wiley-Blackwell are not responsible for the content or functionality of any supporting information supplied by the authors. Any queries (other than missing material) should be directed to the *New Phytologist* Central Office.